ACS OMEGA

http://pubs.acs.org/journal/acsodf

Article

A Novel Cyclic Mobile Transporter Can Induce Apoptosis by Facilitating Chloride Anion Transport into Cells

Goutam Kulsi,[⊥] Achinta Sannigrahi,[⊥] Snehasis Mishra, Krishna Das Saha, Sriparna Datta, Partha Chattopadhyay, and Krishnananda Chattopadhyay*

Cite This: *ACS Omega* 2020, 5, 16395−16405

Read Online

ACCESS | Metrics & More | Article Recommendations | Supporting Information

ABSTRACT: We report here the preparation of an aminoxy amide-based pseudopeptide-derived building block using furanoid sugar molecules. Through the cyclo-oligomerization reaction, we generate a hybrid triazole/aminoxy amide macrocycle using the as-prepared building block. The novel conformation of the macrocycle has been characterized using NMR and molecular modeling studies, which show a strong resemblance of our synthesized compound to D-,L-α-aminoxy acid-based cyclic peptides that contain uniform backbone chirality. We observe that the macrocycle can efficiently and selectively bind Cl^- ion and transport Cl^- ion across a lipid bilayer. ^{1}H NMR anion binding studies suggest a coherent relationship between the acidity of aminoxy amide N−H and triazole C−H proton binding strength. Using time-based fluorescence assay, we show that the macrocycle acts as a mobile transporter and follows an antiport mechanism. Our synthesized macrocycle imposes cancer cell death by disrupting ionic homeostasis through Cl^- ion transport. The macrocycle induced cytochrome c leakage and changes in mitochondrial membrane potential along with activation of family of caspases, suggesting that the cellular apoptosis occurs through a caspase-dependent intrinsic pathway. The present results suggest the possibility of using the macrocycle as a biological tool of high therapeutic value.

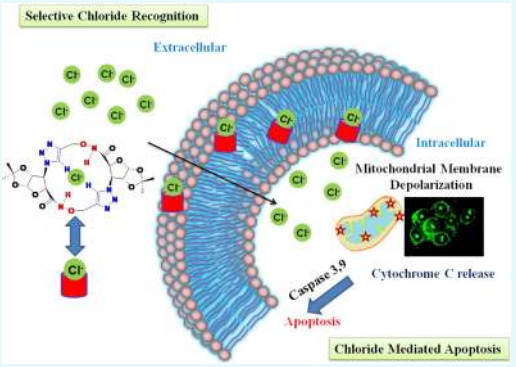

INTRODUCTION

Cellular ion transport systems play crucial roles in different biological processes.[1−5] Malfunctions of endogenous ion channels are responsible for multiple disease conditions, including cystic fibrosis,[5−7] Bartter's syndrome,[8] myotonia,[9] epilepsy,[10] Gitelman syndrome,[11] Dent's disease,[12] renal tubular acidosis,[13] deafness,[14] several neurological disorders, and cancer.[15−18] Artificial channel replacement therapy[19] has been introduced recently for the treatment of the diseases associated with ion channel dysfunctions, in which synthetic anion transporters[18,20−31] are used to replace endogenous malfunctioning ion channels. Though Cl^-, bicarbonate, and phosphate are the most abundant anions in physiological systems,[19] selective transport of Cl^- ions is essential for diverse biological processes, e.g., trans-epithelial salt transport, acidification of internal and extracellular compartments, cell volume regulation, cell cycle, and apoptosis.[17−19]As a result, synthesis of selective and highly efficient chloride ion transporters can be a rational choice for apoptosis-inducing cell death studies. Interestingly, many of the previously reported synthetic ion channels lacked selectivity between chloride and bicarbonate ions. In particular, strongly hydrated bicarbonate was found to bind to O/NH receptors and both the transport of Cl^-/HCO_3^- through NH···anion H bonding was commonly observed by many of the above reports.[29,32−34]

A promising alternative is the CH···anion hydrogen bond. Many groups employed CH···anion interactions for chloride-selective transmembrane anion carriers.[30] One of the popular synthetic strategies involving aminoxy amide-based peptidomimetic macrocycles[35−39] would offer only one binding site toward the ions through their aminoxy amide moiety.

To overcome this limitation, here, we aimed to devise a synthetic strategy that would offer at least an additional C−H binding site (in addition to the popular aminoxy amide) by incorporating a triazole unit.[40−42] The rational for using the C−H site comes from the fact that, in contrast to OH and NH, CH is recognized as a soft H-bond donor.[43−47] It might therefore favor binding to softer, more polarizable anions (e.g., Cl^-) over hard anions such as HCO_3^-.

The execution of the present synthetic strategy comes from several published reports from our laboratory, which involved designing and synthesizing different kinds of triazole-based peptidomimetic macrocycles.[48−51] In addition, we took the

Received: January 31, 2020
Accepted: June 3, 2020
Published: July 2, 2020

Scheme 1. Synthesis of Triazole/Aminoxy Amide-Based Peptidomimetic Macrocycle 10

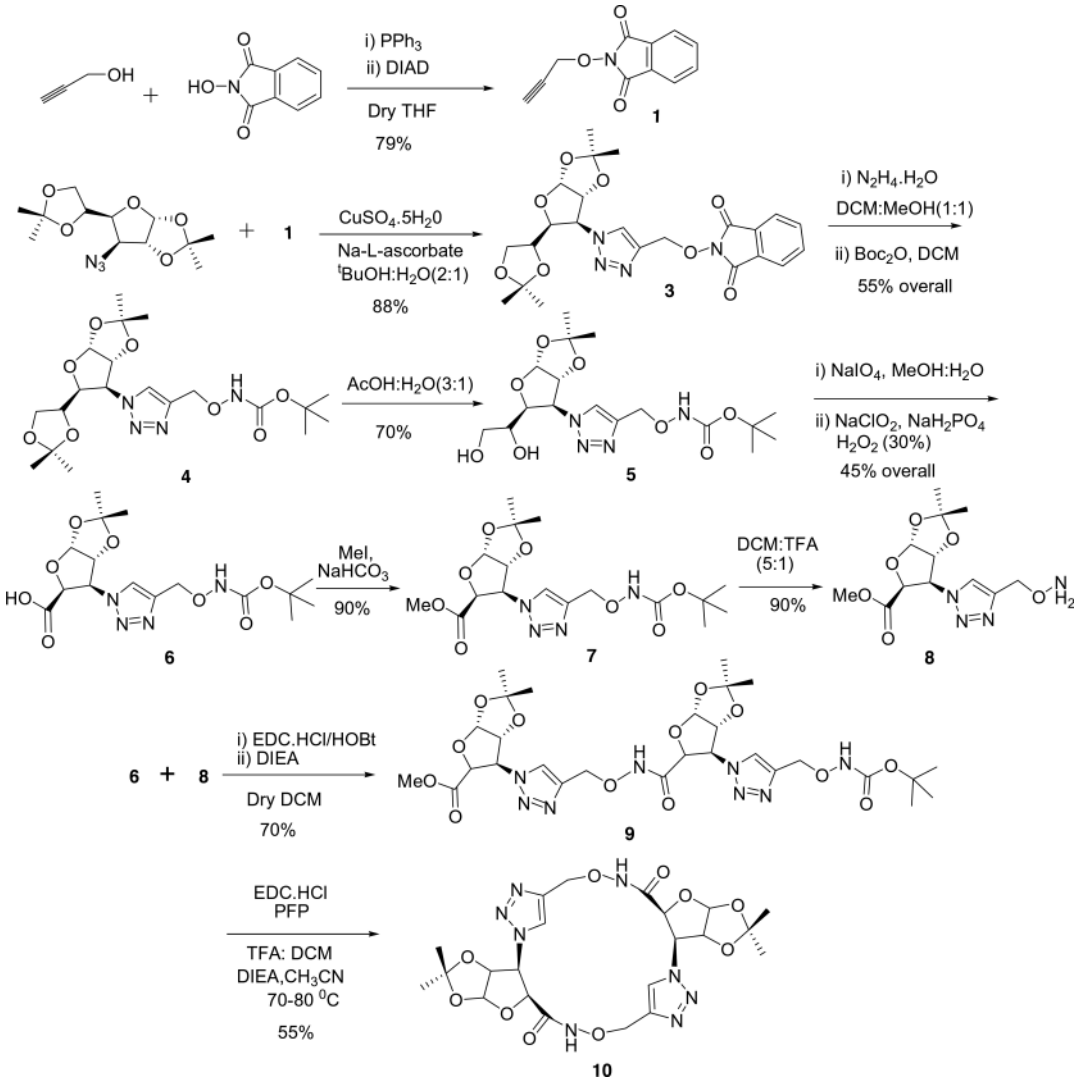

help of available reports using amide and urea moieties as functional groups in the peptide backbone for the construction of these anion-binding artificial ion transporters.[35] The synthesis of a cyclic α-aminoxy/amide-based pseudocyclo-β-peptide having an N-O turn[24,37,38,52] has encouraged us to synthesize a 1,4-linked triazole-modified hybrid triazole/aminoxy amide macrocycle from linear triazoleaminoxy amide-derived oligomers of *cis*-furanoid sugar triazoleaminoxy acid. This is because the higher acidity of CH of (1,4)-linked triazole (a *trans* peptide bond isostere in terms of planarity, polarity, and hydrogen bond donating and accepting capacities) compared to the normal amide NH would allow us to obtain better binders of anions, a property that is crucial for an ion receptor.[38,53−56] In comparison to cyclic α-peptides per amino acid subunit, cyclic β-peptides contain an additional CH_2 group and they are also conformationally more stable than α-peptides. The present study highlights the synthesis of (1,4)-linked triazole-modified aminoxy amide-based cyclic anion receptor (**10**) from propargyl amine and acyclic anion receptor (**18**) from homopropargyl amine (Scheme 1 and Chart 1). We have successfully synthesized the novel peptidomimetic macrocycles incorporating (1,4)-linked triazole over an amide bond surrogate to construct a cyclic anion

Chart 1. (1,4)-Linked Triazole-Modified Aminoxy Amide-Based Cyclic Anion Transporter (10) from Propargyl Amine and Acyclic Anion Transporter (18) from Homo Propargyl Amine

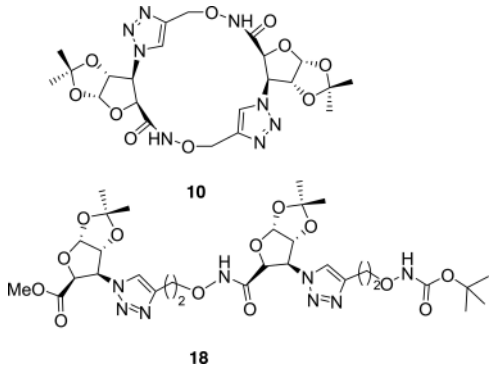

receptor with aminoxy amide functionality without any intramolecular H bond forming any turn (Scheme 1). Our investigations also reveal that replacing the amide bond in an aminoxy amide-based cyclic peptide with a 1,4-triazole linkage leads to a perfect bracelet conformation, resembling the cyclic

https://dx.doi.org/10.1021/acsomega.0c00438
ACS Omega 2020, 5, 16395−16405

hexapeptide of D-,L-α-aminoxy acids having uniform backbone chirality. The anion binding properties of cyclic compound **10** have been studied using the standard ^{1}H NMR spectroscopic method. This NMR method assesses anion binding affinities of the cyclic compound toward anions (for example, Cl^-, Br^-, and I^-). The results reveal that the cyclic compound is not only an effective anion binding agent in solution but also selective toward chloride ion. Regarding compound **18**, our initial aim was to prepare a bigger cyclopeptide that may bind selectively with different anions. To obtain the second compound, i.e., the tetramer **18**, β-aminoxyhomopropargyl amine has been used instead of propargyl amine and the rest of the synthesis has been similar to the above procedure (see the Supporting Information). However, the result has differed from the previous one in the last step so far as the cyclization does not occur. This is probably because of the formation of a secondary N-O turn by the tetramer.

We have subsequently investigated if this macrocycle would act as an anion transporter. For that purpose, we have synthesized large unilamellar vesicles (LUVs) composed of egg PC (phosphatidylcholine) to study the Cl^- influx into liposomes by monitoring the fluorescence intensity of an entrapped Cl^--sensitive indicator, 6-methoxy-*N*-(3-sulfopropyl) quinolinium (SPQ).[57] A rapid decrease in the fluorescence of SPQ suggests that the macrocycle transports Cl^- into the liposomes. We have also verified the selectivity of **10** for Cl^- with respect to the HCO_3^- ions. Finally, we have performed experiments using different concentrations of cholesterol to confirm that transport has been occurring via the "mobile carrier" mechanism in an antiport manner (Figure 1). The

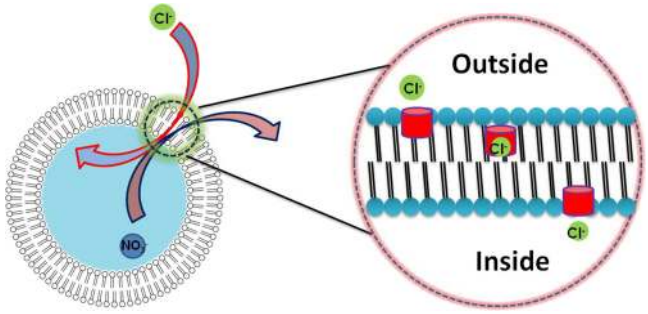

Figure 1. Anion transport was monitored by fluorescence quenching of SPQ-loaded LUVs as a result of the interaction of chloride ions with internal SPQ in vesicles as a mobile carrier mechanism.

strong Cl^- ion transportation properties of both aminoxy amide and the triazole unit of compound **10** have prompted us to explore their anticancer activity inside live cells. By live cell microscopy, FACS (fluorescence-activated cell sorting), mitochondria depolarization, and other assays, we have shown that the transport of Cl^- into HCT 116 cells by compound **10** facilitates the activation of caspase-dependent apoptotic pathways.

RESULTS AND DISCUSSION

Synthesis of the Peptidomimetic Macrocycle and Acyclic Tetramer. The target triazole/aminoxy amide macrocycle (compound **10**) was synthesized using Scheme 1. As shown in Scheme 1, the Cu(I)-catalyzed cyclo-addition between *O*-phthalimide-protected propargyl alcohol (**1**) and 3-azido-(1,2:5,6)-diisopropylidene glucose (**2**) resulted in the formation of the central intermediate (**3**).[58,59] The Boc-protected triazoleaminoxy amine (**4**) was then synthesized by phthalimide deprotection using hydrazine hydrate, which was followed by Boc protection under mild conditions. After deprotection of the isopropylidene derivative by AcOH:H_2O (3:1), oxidation of diol with sodium periodate cleavage furnished the aldehyde, which was again oxidized to Boc-protected sugar triazole amino acid (**6**). As shown in Scheme 1, the major intermediate (**6**) was subjected to iterative protection and deprotection via acid treatment, which yields compound **8**. The EDC/HOBt coupling between (**6**) and (**8**) resulted in a linear tetramer (**9**). After the hydrolysis of linear tetramer (**9**) by LiOH·H_2O, the compound was activated by the formation of penta-fluorophenyl ester, which was subjected to peptide coupling to yield the cyclic peptide (**10**) (Scheme 1).[46−49] To obtain the second compound, i.e., the tetramer (**18**), β-aminoxy homopropargyl amine was used instead of propargyl amine and the rest of the synthesis was similar to the above procedure. However, the result differed from the previous one in the last step so far as the cyclization did not occur. This is probably because of the formation of a secondary N-O turn by the tetramer.

Conformational Analysis. To determine the molecular structure and conformation of **10**, we used NMR and molecular modeling (Figure 2). The ^{1}H NMR spectra of **10**

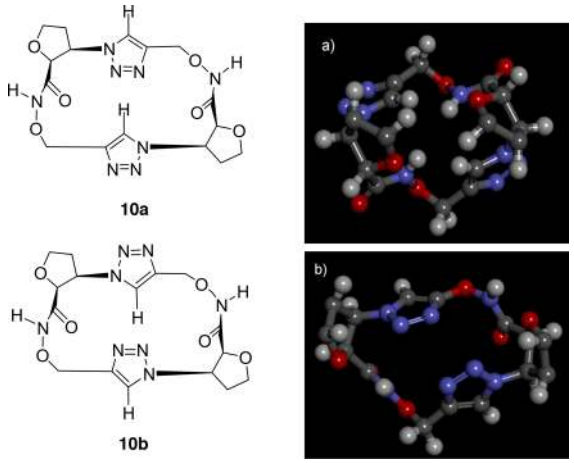

Figure 2. Two possible lowest energy conformations of triazole/aminoxy-based peptidomimetic macrocycle **10**. (a) Structure resembling the D-,L-α-aminoxy acid-based cyclic peptides. (b) Structure resembling aminoxy/amide-based hybrid cyclic peptides.

in both polar and nonpolar solvent ($CDCl_3$) suggested that the compound has an averaged C_2 symmetry. The weak intensity of ROE cross peaks between the signals of triazole and adjacent Cβ proton of sugar indicated pseudo-*trans*-amide conformation in the backbone of **10**. The observed JCαH and CβH of the furanoid sugar component (~4 Hz) indicated the presence of a gauche conformation of the sugar moiety in **10**. Molecular modeling and ROESY (rotating frame overhause effect spectroscopy) revealed that compound **10** tends to minimize nonbonded intramolecular side chain−side chain and side chain−backbone interactions by C_2 symmetric bracelet conformation with a possible pore size of 3.8 Å.[38,39,50] The aminoxy amide NH and triazole CH protons pointed inward while the side chains remained outward, which was similar to the anion binding D-,L-α-aminoxy acid-based cyclic peptides as observed before.[39] The slightly turned structure was also characterized by FTIR spectroscopy, which

https://dx.doi.org/10.1021/acsomega.0c00438
ACS Omega 2020, 5, 16395−16405

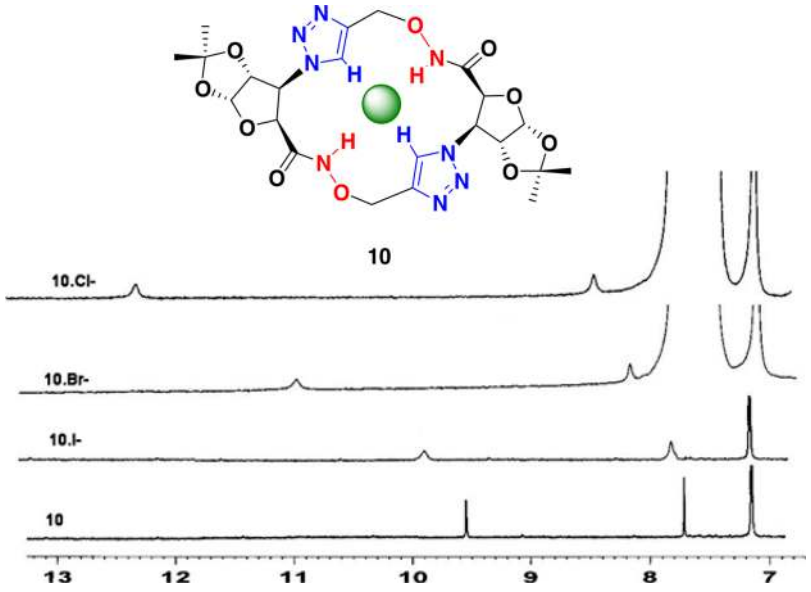

Figure 3. Downfield ^{1}HNMR shift of both triazole CH and aminoxy amide NH of peptidomimetic macrocycle **10** with Ph_4PCl, Ph_4PBr, and TBAI in $CDCl_3$. For possible complexation, a significant downfield shift was observed upon the addition of 10 equiv of guest anion with 3 mM concentration of compound **10**.

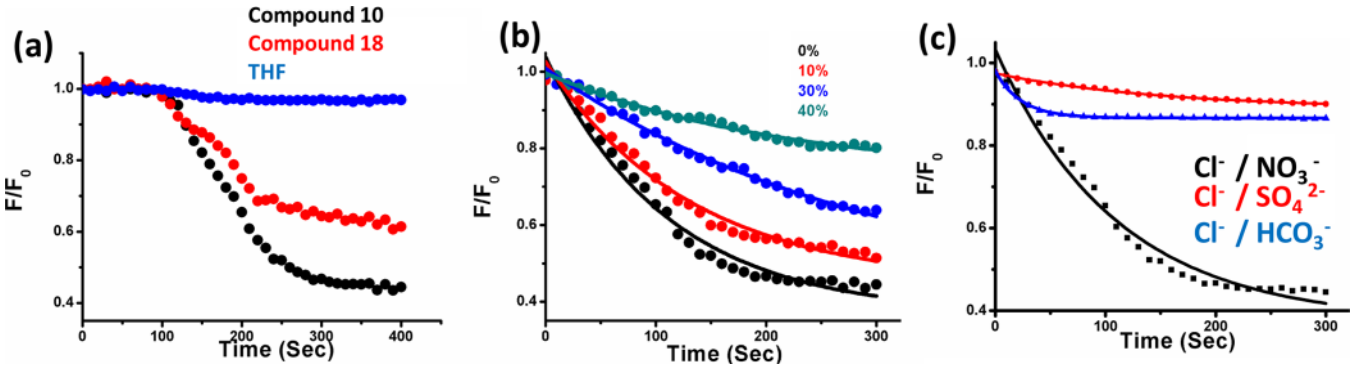

Figure 4. Chloride ion transport into liposomes using time-based fluorescence decay measurements. Inside the vesicles: 200 mM $NaNO_3$, 0.5 mM SPQ. Outside the vesicles: 200 mM NaCl. (a) At 100 s, compound **10** (cyclic compound) and compound **18** (acyclic compound) were added. (b) Chloride transport by macrocycle **10** through the LUVs containing different percentages of cholesterol. (c) Exchange of chloride by different anions (SO_4^{2-} and HCO_3^-) showing the antiporter activity. For all the experiments, the typical concentrations of the compounds were taken (5 μM).

showed the presence of an aminoxy amide N−H peak at 3280 cm^{-1}. This N−H peak was found lower than that of a typical nonhydrogen-bonded aminoxy amide N−H (3400−3380 cm^{-1}), indicating the involvement of intermolecular hydrogen bonding of the aminoxy amide.[38,39] ^{1}H NMR spectral data ($CDCl_3$) were assigned from the corresponding 2D double-quantum-filtered (DQF)-COSY and ROESY spectra. Due to the bracelet-like conformation with small pore size, we assumed that compound **10** may bind small ions. It is to be noted that the effect of size variation as a result of triazole incorporation could not be ruled out.

Anion Binding Property. To validate the above assumption on the ion binding property of **10**, we used ^{1}H NMR. The ^{1}H NMR spectrum in $CDCl_3$ displayed two well-separated singlets at δ = 9.59 and 7.55 ppm corresponding to aminoxy amide and triazole CH protons, respectively. In the presence of added chloride ions, we observed significant downfield shifts for both aminoxy amide (>2.9 ppm) and triazole (>1.2 ppm) protons.[51] This data suggested possible involvement of both aminoxy amide and triazole moieties in chloride binding. This bidendate binding character is possible because of the bracelet conformation of compound **10**, a result validated also by molecular modeling. Moreover, the sum of the van der Waals radii of chloride (∼1.8 Å) is close to the possible cavity size of the macrocyle **10**. This is one of the reasons for the chloride selectivity of compound **10** over others anions. It may be noted that an upfield shift (and not downfield as observed here) of aminoxy amide proton was observed before in the case of aminoxy/amide-based cyclic peptides.[37,39] We also observed a large line broadening for both resonances in the presence of chloride ion, which is consistent with binding dynamics occurring in the NMR timescale, as noted before.[39] Other anions, like bromide or iodide, were also found to bind with **10** (Figure 3). From the ^{1}H NMR shift in Figure 3, we estimated that the binding followed the order $Cl^- > Br^- > I^-$.

Ion Transport Activities through Liposome. We wanted to determine if **10** and **18** were able to transport chloride ions across synthetic liposomes. For this assay, we prepared egg-PC LUVs containing a Cl^- sensitive indicator, 6-methoxy-*N*-(3-sulfopropyl) quinolinium (SPQ). The fluorescence of SPQ would decrease once chloride ions are

https://dx.doi.org/10.1021/acsomega.0c00438
ACS Omega 2020, 5, 16395−16405

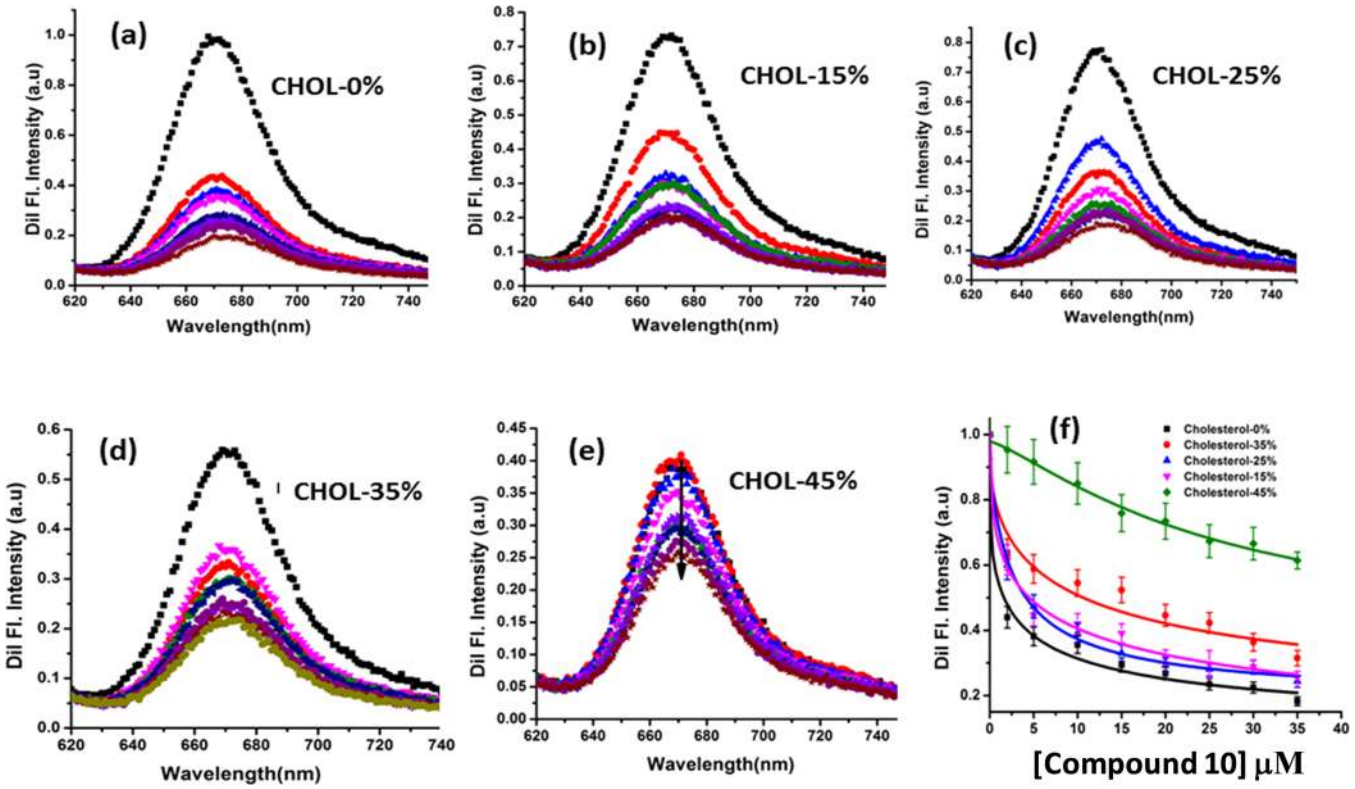

Figure 5. Fluorescence titration experiments using DiI-C18-labeled egg-PC LUVs composed of (a) 0%, (b) 15%, (c) 25%, (d) 35%, and (e) 45% cholesterol. (f) DiI C-18 fluorescence intensities were plotted against the concentration of macrocyclic compound **10** to obtain the binding constants.

transported from the outside into the vesicles. In the absence of **10** and **18**, no change in fluorescence intensity was observed for SPQ. In contrast, the presence of **10** and **18** resulted in a large decrease in fluorescence intensity with time (Figure 4), which occurred as chloride ions entered inside the vesicles. It was interesting to note that the rate and extent of the reduction in fluorescence intensity were found to be significantly higher for **10** in comparison to **18**, which further indicated the better transport efficacy of **10** (Figure 4a). We found out that the transport of bicarbonate was significantly less compared to that of chloride, which established chloride selectivity (Figure 4c).

We then wanted to find out if **10** can act as an antiporter by exchanging chloride for intravesicular nitrate (as shown in Figure 4). To determine that, we used a published method by SPQ assay. We found that **10** transported chloride when nitrate was present inside the vesicles, but no chloride transport activity was observed with sulfate, replacing nitrate in the intravesicular space. Finally, we performed experiments to confirm that the transport was occurring via the "mobile carrier" mechanism (Figure 4b) and not by self-assembly into channels. SPQ assay (Cl^-/NO_3^- exchange) was conducted to **10** using vesicles prepared with different levels of cholesterol. An increase in cholesterol concentration decreased membrane fluidity, restricting the movement of the carrier molecule. As expected, the transport rate decreased dramatically when the proportion of cholesterol was raised to 40% (see the Supporting Information). The dependence of transport rates on the loading concentration of **10** is plotted in Figure 5. In addition, the binding between **10** and egg-PC LUVs decreased as we increased cholesterol concentrations in the membrane (Figure 5 and Table 1).

Table 1. Binding Constants and Co-operative Indices of Macrocyclic Compound 10 with LUVs Composed of Egg PC Containing Different Molar Percentages of Cholesterol

systems	association constants (K_a, M^{-1})	co-operative indices (n)
egg-PC-chol-0%-cyclic compound	$2.77(\pm0.16) \times 10^5$	0.58
egg-PC-chol-15%-cyclic compound	$2.42(\pm0.07) \times 10^5$	0.86
egg-PC-chol-25%-cyclic compound	$1.55(\pm0.05) \times 10^5$	0.53
egg-PC-chol-35%-cyclic compound	$0.99(\pm0.02) \times 10^5$	0.62
egg-PC-chol-45%-cyclic compound	$0.38(\pm0.06) \times 10^5$	1.25

To investigate if the binding of **10** and **18** with egg-PC LUVs resulted in any change in membrane physical property, we used FTIR spectroscopy. The egg PC sample in the absence of **10** and **18** was characterized by two vibrational frequency maxima positioned at 2855 and 2923 cm^{-1} (see the Supporting Information). When **10** was added, these peak maxima shifted to 2887 and 2975 cm^{-1}, respectively, indicating a change in the symmetric CH_2 vibrational frequency of the hydrocarbon component of egg PC. In addition, the carbonyl bond frequency (1730 cm^{-1}) of egg PC shifted to 1734 $cm^{-1}$when we added **10**. Also, a significant decrease in H-bonded ester carbonyl vibrational frequency (1728 cm^{-1}) and substantial enhancement of nonhydrogen-bonded carbonyl stretching vibration (1742 cm^{-1}) occurred when **10** was added to egg-PC LUVs (Figure 6). FTIR suggested the significant interaction of **10** with the carbonyl group of egg PC. Similar alterations in vibrational modes of different bonds were

https://dx.doi.org/10.1021/acsomega.0c00438
ACS Omega 2020, 5, 16395−16405

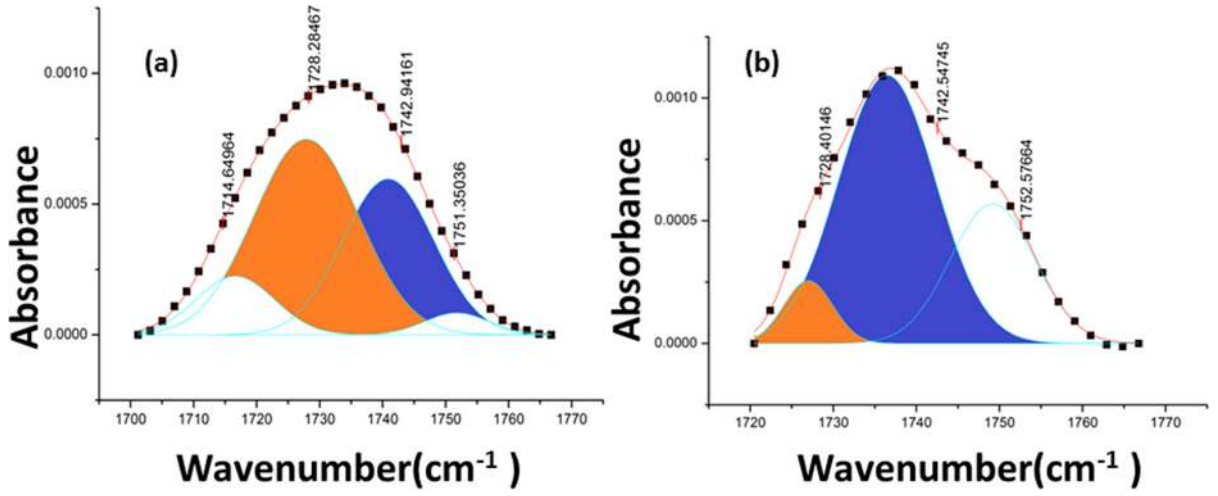

Figure 6. Deconvoluted FTIR spectral signatures of ester carbonyl stretching vibrations of egg PC in the (a) absence and (b) presence of macrocyclic compound **10**. In the presence of macrocyclic compound, the extent of nonhydrogen-bonded carbonyl frequency (1728 cm^{-1}) decreases with a concomitant increase in hydrogen-bonded carbonyl frequency (1742 cm^{-1}).

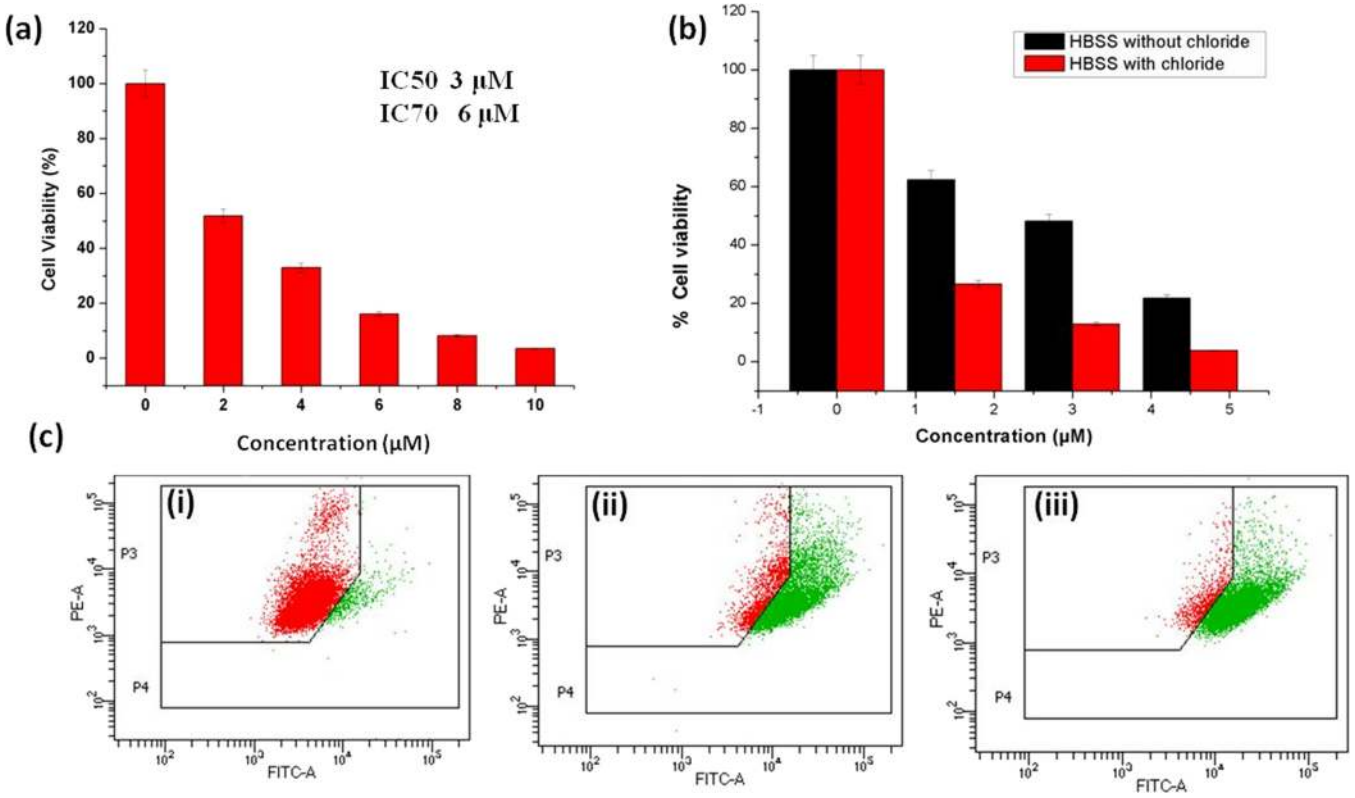

Figure 7. (a) Cell viability obtained after 12 h treatment of compound **10** (0−10 μM each) against HCT 116 by MTT assay. (b) Comparison of HeLa cell viability in Cl^--containing and Cl^--free HBSS buffer upon dose-dependent treatment of **10** (0−5 μM) for 24 h. (c) Flow cytometric analysis of HCT 116 cells untreated (control, i) and treated with 3 μM (ii) and 6 μM (iii) compound **10** for 12 h and stained with JC-1.

observed also in presence of **18** (see the Supporting Information).

Ion Transport Activity of the Macrocycle in the Cellular Environment. Cellular apoptosis can take place due to the disruptions of cellular ionic homeostasis by Cl^- ion transportation resulting in a change in pH. Recent reports show that artificial Cl^- ion transporters can kill the cancer cells in the apoptotic pathway by disrupting the cellular ionic equilibrium. The significant Cl^- ion transportation activities of both aminoxy amide and the triazole unit of **10** motivated us to examine their functions in the cellular environment. The viability of **10** was examined in human colorectal carcinoma (HCT 116) cell line by MTT assay at different concentrations (0−10 μM). The viable cell population was found to be decreased gradually with increasing concentrations of **10** (Figure 7a). The IC50 and IC70 values for **10** were 3 and 6 μM, respectively, for HCT 116 cell line (Figure 7a). To study whether the cell death by **10** is because of the alteration in Cl^- ion concentration in the cellular environment, MTT assay was carried out in the absence and presence of Cl^- ion using the

https://dx.doi.org/10.1021/acsomega.0c00438
ACS Omega 2020, 5, 16395−16405

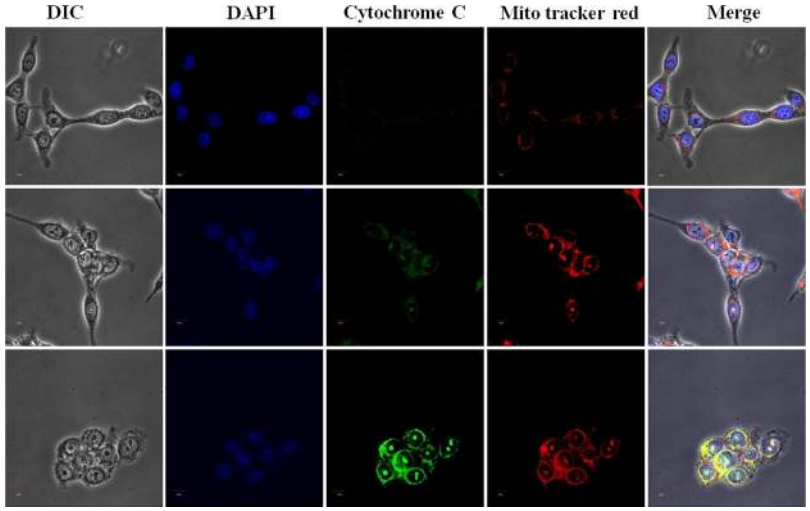

Figure 8. Confocal microscopy study of cytochrome C release after treatment of compound **10** at 3 and 6 μM concentrations in the presence of DAPI and MitoTracker red. Treatment duration was for 12 h.

HBSS (Hank's balanced salt solution) buffer. In the presence of compound **10**, higher viable cell population was found in the case of the HBSS buffer without Cl^- ion. In contrast, cell viability was significantly dropped when Cl^- ions were present (Figure 7b). This result indicates that intracellular Cl^- ion transport by compound **10** is associated with the percentage of cell death in a direct manner. In particular, the cellular apoptosis pathway has been triggered by Cl^- ion transportation. A chronological change that occurs in the cells during the apoptotic pathway can be studied by observing several cellular processes during apoptosis: (a) mitochondrial membrane integrity through flow cytometry analysis, (b) alterations in cellular architecture and release of cytochrome c as revealed by confocal imaging, and (c) mechanistic study on the apoptosis pathways are those examples. Significant morphological changes including cell shrinkage was observed when HCT 116 cells were incubated with compound **10** (Figure 8), and the effect was prominent with an increase in dose. These studies suggested the cell death through apoptosis. The pre-apoptosis activity was measured by the disruption of mitochondrial membrane potential (MMP) that can be monitored by using JC-1, a membrane potential-sensitive dye. The green fluorescence signal due the JC-1 dye diffusion in the cytosol was a consequence from the depolarization of the mitochondrial membrane. HCT 116 cells were incubated with compound **10** for 24 h, and the staining of the cells was done with JC-1 dye (Figure 7c). We observed a stepwise increase in JC-1 dye green fluorescence signals with respect to the change in concentration, suggesting the MMP in the presence of compound **10**.

Apoptosis can also be instigated by a caspase-mediated extrinsic pathway. However, caspase-9 activate caspase-3, a common effector and essential intermediate among all caspases. In this regard, the expressions of the caspase enzymes in the HCT 116 cells were examined by colorimetric assay for the determination of the apoptosis pathway of compound **10**. The expression levels of initiator caspase-9 and caspase-3 were explored in the presence of compound **10** in a dose-dependent manner (0−6 μM). Here, we found that the expression of caspase-9 and caspase-3 has been increased in a dose-dependent manner (Figure 9). The level of caspase-9 and caspase-3 further inferred the caspase-dependent intrinsic pathway of apoptosis in the presence of compound **10** (Figure 9).

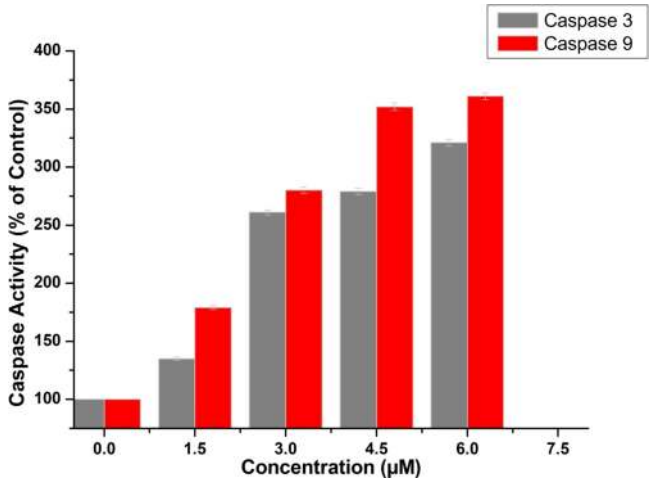

Figure 9. Expression of caspase-3 and caspase-9 after the treatment of compound **10** at different concentrations for 12 h.

CONCLUSIONS

The present study describes the synthesis of an aminoxy amide-based pseudopeptide-derived building block from furanoid sugar molecules and its use to generate a hybrid triazole/aminoxy amide macrocycle by cyclo-oligomerization. We established, by NMR and molecular modeling studies, the conformation of the novel triazole/aminoxy amide macrocycle, which resembled the D-,L-α-aminoxy acid-based cyclic peptides with uniform backbone chirality. It is an electroneutral receptor, and its anion binding properties demonstrated its great potential to be an effective anion receptor. The macrocycle is an interesting scaffold for ion transport as it is able to discriminate between various anions and shows a preference for chloride ion. This novel macrocyclic compound remarkably affects the chloride/nitrate exchange process in LUVs as monitored by the reduction in fluorescence of SPQ entrapped in vesicles. In addition, the strong Cl^- ion transportation property of both aminoxy amide and the

https://dx.doi.org/10.1021/acsomega.0c00438
ACS Omega 2020, 5, 16395−16405

triazole unit of compound **10** is responsible for anticancer activity of **10** inside live cells. Triazole CH is recognized as a soft H-bond donor that favored selective chloride binding. In view of aminoxy amide protons being excellent hydrogen bond donors, we believe that aminoxy acids would be useful building blocks for various anion receptors with practical applications. This system could be used as a biological tool that may replace defective chloride transporter in living systems.

EXPERIMENTAL SECTION

SPQ-Loaded Liposome Preparation. The required amount of egg PC (91 mg) in chloroform was transferred to a 10 mL glass bottle. Lipid film was made by removal of organic solvent through passing dry nitrogen gas in a gentle manner. The sample was then placed in a desiccator connected to a vacuum pump for overnight drying. A solution of 200 mM $NaNO_3$ and 0.5 mM SPQ (1.2 mL) was added to the dried lipid film to obtain our desired final concentration (10 mM). Vortexing of the hydrated lipid film for about 30 min produced multilamellar vesicles (MLVs). LUVs were prepared by extruding the MLV with a LiposoFast AVESTIN extruder (Ottawa, Canada). The MLV suspensions were extruded through polycarbonate membranes having pore diameters of 120 nm, which resulted in the formation of LUVs (average diameter ≈ 120 nm) with well-defined sizes, as measured by dynamic light scattering (DLS). The LUV suspension was separated from extra vesicular dye by size exclusion chromatography. The vesicle solutions were degassed prior to all measurements, as air bubbles introduced into the sample during extrusion may lead to artifacts. Large unilamellar vesicles (LUVs) composed of egg PC with different molar percentages of cholesterol were prepared following the abovementioned protocol.

Fluorescence Assay. Typically, 100 μL of SPQ-loaded vesicles (stock solution) was suspended in 1.9 mL of solution C (200 mM NaCl) and placed in a fluorimetric cell. SPQ emission at 430 nm was monitored using an excitation wavelength of 360 nm. At 100 s, 20 μL of a 5 μM THF solution of compound **10** (cyclic compound) and compound **18** (acyclic compound) were added through an injection port. Time-based fluorescence spectra were taken using a PTI (Photon Technology International Inc.) fluorimeter. For normalizing the data, all fluorescence values (F) were divided by the fluorescence value obtained before the addition of compound (F_0). At the end of the experiments, triton X-100 was added in each of the liposome samples.

FTIR. FTIR samples were prepared by drop-casting a concentrated aqueous dispersion of LUVs composed of egg PC on a glass slide and then drying in an oven at 45 °C for 2 h. The dried film on glass was then placed in the machine's sample chamber. FTIR spectra of egg PC and egg PC in the presence of compound **10** and **18** were measured using a Bruker Tensor 27 FTIR spectrometer. The FTIR spectral readouts were taken in water. Water baseline was subtracted before taking each spectrum. To study the structural changes of the lipid bilayer, we studied the alterations in frequencies at ∼3000 for symmetric stretching mode of CH_2 and 1700−1800 for C═O stretching mode.

Dynamic Light Scattering (DLS). The hydrodynamic radius of the liposomes was measured using DLS experiments.[60,61] In the DLS experiments, the intensity fluctuations of scattered light were measured and the intensity autocorrelation function was fit to the exponential decay function to obtain the values of the diffusion coefficient (D). The Einstein−Stokes relation

$$a = kT/6\pi\eta D \quad (1)$$

was used to calculate the hydrodynamic radius of the vesicle. D is the diffusion constant, and kT is the thermal energy. For size measurements, a 100 μM concentration of egg PC was used.

Binding Assay Using Fluorescence Spectroscopy. We used fluorometric assay for studying the binding of the macrocyclic compound with LUVs composed of egg PC containing different molar percentages of cholesterol (0, 15, 25, 35, and 45%). All samples were prepared in 20 mM sodium phosphate buffer at pH 7.4. A set of samples was prepared using a 1 mM concentration of uniformly synthesized lipid vesicles. In each sample vial, 0.5 wt % membrane-specific DiI C-18 dye was added, and the samples were kept at 37 °C for overnight incubation.[62] Subsequently, the required amount of macrocyclic compound **10** was added gradually. The samples were then incubated at 25 °C for 2 h. The steady-state fluorescence emission spectra of the dye were recorded at an excitation wavelength of 600 nm. The peak intensity values at 671 nm for egg PC were plotted with macrocyclic compound concentrations. The data were fit using the sigmoidal Hill equation as follows

$$F = F_0 + \frac{(F_e - F_0)x^n}{(x^n + K^n)} \quad (2)$$

where F and F_0 refer to the fluorescence intensities of DiI C-18 in the presence and absence of macrocyclic compound, respectively. F_e denotes the minimum intensity in the presence of a higher concentration of compound, and K is the equilibrium dissociation coefficient of the lipid−compound complex. n is the Hill coefficient, which measures the cooperativity of binding, and x is the concentration of the macrocyclic compound. The PTI fluorimeter (Photon Technology International, Inc) and a cuvette with a 1 cm path length were used for the fluorescence measurements.[63]

Cell Lines and Chemicals. Human colorectal carcinoma (HCT 116) cell line was obtained from the National Center for Cell Sciences (NCCS), Pune, India. Cell culture media components, viz., Dulbecco's modified eagle medium (DMEM), penicillin−Streptomycin−neomycin (PSN) antibiotic cocktail, fetal bovine serum (FBS), trypsin, and ethylenediaminetetraacetic acid (EDTA), were obtained from Gibco (Grand Island, NY, USA). Additional raw and fine chemicals were procured from Sisco Research Laboratories (SRL), Mumbai, India, and Sigma-Aldrich, St. Louis, MO, USA, respectively. Dyes were procured from Thermo Fisher Scientific − US. Antibodies were bought from Santa Cruz Biotechnology, Dallas, Texas, USA, and Bioscience, San Diego, USA.

Cell Culture and Cytotoxicity Assay. HCT 116 cells were cultured in DMEM accompanied with 10% fetal bovine serum (FBS) and 1% antibiotic (PSN) under 5% CO_2 in a humidified atmosphere at 37 °C. After 75−80% confluence, cells were harvested with 0.52 mM EDTA and 0.25% trypsinin phosphate buffered saline (PBS) and plated at the required density to allow them to re-equilibrate for a day before starting the experiment.[64] MTT assay was directed to evaluate the cell cytotoxicity.[65] For the initial screening experiment, the HCT 116 cells (4×10^3 cells per well) were seeded in a 96 well plate and left in an incubator followed by treatment with different

https://dx.doi.org/10.1021/acsomega.0c00438
ACS Omega 2020, 5, 16395−16405

concentrations of compound **10** (0−10 μM) for 12 h. After 12 h of incubation, cells were washed with PBS, and then the MTT solution was added to each well and kept in an incubator for 4 h to form formazansalt. Cellular media was replaced by HBSS buffer (either with Cl^-or without Cl^-) containing 10% FBS. Then, the formazan salt was solubilized using DMSO and the absorbance was observed at 595 nm using an ELISA reader (Emax, Molecular Devices, USA). Simultaneously, one other set of 96 well plate was taken for MTT assay, where cellular medium was replaced by HBSS buffer (either with Cl^- or without Cl^-) containing 10% FBS.

Measurement of Mitochondrial Membrane Potential Using Flow Cytometry. Cationic carbocyanine dye, JC-1 (5,5′,6,6′-tetrachloro-1,1′,3,3′-tetraethyl benzimidazolyl carbocyanine iodide), was used to measure mitochondrial membrane potential. Treated cells were incubated with the cationic carbocyanine dye, JC-1, followed by flow cytometric analysis according to the manufacturer protocol. JC-1 displays potential-dependent accumulation in mitochondria and demonstrates a fluorescence emission shift from green (525 nm) to red (590 nm). The fluorescence change, therefore, allows determining the percentage of depolarized and hyperpolarized mitochondria on the basis of the resultant fluorescence of the JC-1 monomer and aggregate.[18]

Immuno-fluorescence. Control/treated HCT 116 cells were washed two times for 10 min each in PBS (0.01 M) and incubated for 1 h in blocking solution containing 2% normal bovine serum and 0.3% triton X-100 in PBS. After blocking, the cells were incubated overnight at 4 °C with the cytochrome C antibody followed by washing and incubation with respective fluorophore-conjugated secondary antibodies (anti-rabbit FITC) for 2 h. The slides were then counterstained with 6-diamidino-2-phenylindole (DAPI) and MitoTracker Red for 10 min and mounted with the ProLong Antifade Reagent (Molecular Probe, Eugene, OR, USA).[66] Stained cells were examined using a confocal laser-scanning microscope (FV 10i, Olympus, Japan).

Measurement of Caspase-3 and Caspase-9 Activities. Caspase-3/9 activities were measured according to the manufacturer's directions with commercially existing caspase-3 and caspase-9 colorimetric assay kits (BioVision Research Products, Mountain View, CA). Absorbance was measured at 405 nm using an ELISA reader.

■ ASSOCIATED CONTENT

Supporting Information

The Supporting Information is available free of charge at https://pubs.acs.org/doi/10.1021/acsomega.0c00438.

Detailed synthetic scheme and procedures, supporting figures, table, and NMR spectra, FTIR characterization, liposome preparation, molecular modeling, and multi-dimensional NMR (PDF)

■ AUTHOR INFORMATION

Corresponding Author

Krishnananda Chattopadhyay − *Structural Biology and Bioinformatics Division, CSIR- Indian Institute of Chemical Biology (IICB), Kolkata 700032, India;* orcid.org/0000-0002-1449-8909; Email: krish@iicb.res.in

Authors

Goutam Kulsi − *Structural Biology and Bioinformatics Division and Organic and Medicinal Chemistry Division, CSIR- Indian Institute of Chemical Biology (IICB), Kolkata 700032, India*

Achinta Sannigrahi − *Structural Biology and Bioinformatics Division, CSIR- Indian Institute of Chemical Biology (IICB), Kolkata 700032, India*

Snehasis Mishra − *Cancer Biology and Inflammatory Disorder Division, CSIR- Indian Institute of Chemical Biology (IICB), Kolkata 700032, India; Department of Chemical Technology, University of Calcutta, Kolkata 700009, India*

Krishna Das Saha − *Cancer Biology and Inflammatory Disorder Division, CSIR- Indian Institute of Chemical Biology (IICB), Kolkata 700032, India*

Sriparna Datta − *Department of Chemical Technology, University of Calcutta, Kolkata 700009, India*

Partha Chattopadhyay − *Organic and Medicinal Chemistry Division, CSIR- Indian Institute of Chemical Biology (IICB), Kolkata 700032, India*

Complete contact information is available at: https://pubs.acs.org/10.1021/acsomega.0c00438

Author Contributions

$^{\perp}$G.K. and A.S. contributed equally. G.K. synthesized and characterized all compounds and performed anion binding, conformational analysis, and molecular modeling study. A.S. contributed to ion transport activity. S.M. performed in vitro experiments. G.K., A.S., and S.M. analyzed respective data. P.C. and G.K. designed schemes. K.C., P.C., K.D.S., and S.D. supervised respective fields. K.C. wrote the introduction part and supervised the overall project. The manuscript was written through contributions of all authors.

Notes

The authors declare no competing financial interest.

■ ACKNOWLEDGMENTS

We thank the Central Instrumentation Facility of CSIR-IICB for the provision of infrastructure and the Director for his encouragements.

■ REFERENCES

(1) Zhao, F.; Zhao, Y.; Liu, Y.; Chang, X.; Chen, C.; Zhao, Y. Cellular uptake, intracellular trafficking, and cytotoxicity of nanomaterials. *Small* **2011**, *7*, 1322−1337.

(2) Chen, S.; Tang, Y.; Zhan, K.; Sun, D.; Hou, X. Chemiresistive nanosensors with convex/concave structures. *Nano Today* **2018**, 84.

(3) Teyssandier, J.; De Feyter, S.; Mali, K. S. Host−guest chemistry in two-dimensional supramolecular networks. *Chem. Commun.* **2016**, *52*, 11465−11487.

(4) Gale, P. A.; Quesada, R. Anion coordination and anion-templated assembly: highlights from 2002 to 2004. *Coord. Chem. Rev.* **2006**, *250*, 3219−3244.

(5) Das, R. N.; Kumar, Y. P.; Schütte, O. M.; Steinem, C.; Dash, J. A DNA-Inspired Synthetic Ion Channel Based on G−C Base Pairing. *J. Am. Chem. Soc.* **2015**, *137*, 34−37.

(6) Reiner, J. E.; Balijepalli, A.; Robertson, J. W. F.; Campbell, J.; Suehle, J.; Kasianowicz, J. J. Disease detection and management via single nanopore-based sensors. *Chem. Rev.* **2012**, *112*, 6431−6451.

(7) Shen, B.; Li, X.; Wang, F.; Yao, X.; Yang, D. A synthetic chloride channel restores chloride conductance in human cystic fibrosis epithelial cells. *PLoS One* **2012**, *7*, No. e34694.

(8) Amirlak, I.; Dawson, K. Bartter syndrome: an overview. *Qjm* **2000**, *93*, 207−215.

(9) Koch, M. C.; Steinmeyer, K.; Lorenz, C.; Ricker, K.; Wolf, F.; Otto, M.; Zoll, B.; Lehmann-Horn, F.; Grzeschik, K. H.; Jentsch, T. J. The skeletal muscle chloride channel in dominant and recessive human myotonia. *Science* **1992**, *257*, 797−800.
(10) Penfield, W.; Jasper, H., *Epilepsy and the functional anatomy of the human brain*; Little, Brown & Co., 1954.
(11) Cruz, D. N.; Shaer, A. J.; Bia, M. J.; Lifton, R. P.; Simon, D. B. Gitelman's syndrome revisited: an evaluation of symptoms and health-related quality of life. *Kidney Int.* **2001**, *59*, 710−717.
(12) Piwon, N.; Günther, W.; Schwake, M.; Bösl, M. R.; Jentsch, T. J. ClC-5 Cl–channel disruption impairs endocytosis in a mouse model for Dent's disease. *Nature* **2000**, *408*, 369.
(13) Rodriguez Soriano, J. Renal tubular acidosis: the clinical entity. *J. Am. Soc. Nephrol.* **2002**, *13*, 2160−2170.
(14) Myklebust, H. R., *The psychology of deafness: Sensory deprivation, learning, and adjustment*; Grune & Stratton, 1960.
(15) Fürstner, A. Chemistry and biology of roseophilin and the prodigiosin alkaloids: a survey of the last 2500 years. *Angew. Chem., Int Ed.* **2003**, *42*, 3582−3603.
(16) Saha, T.; Gautam, A.; Mukherjee, A.; Lahiri, M.; Talukdar, P. Chloride Transport through Supramolecular Barrel-Rosette Ion Channels: Lipophilic Control and Apoptosis-Inducing Activity. *J. Am. Chem. Soc.* **2016**, *138*, 16443−16451.
(17) Busschaert, N.; Park, S.-H.; Baek, K.-H.; Choi, Y. P.; Park, J.; Howe, E. N. W.; Hiscock, J. R.; Karagiannidis, L. E.; Marques, I.; Félix, V.; Namkung, W.; Sessler, J. L.; Gale, P. A.; Shin, I. A synthetic ion transporter that disrupts autophagy and induces apoptosis by perturbing cellular chloride concentrations. *Nat. Chem.* **2017**, *9*, 667.
(18) Ko, S.-K.; Kim, S. K.; Share, A.; Lynch, V. M.; Park, J.; Namkung, W.; Van Rossom, W.; Busschaert, N.; Gale, P. A.; Sessler, J. L.; Shin, I. Synthetic ion transporters can induce apoptosis by facilitating chloride anion transport into cells. *Nat. Chem.* **2014**, *6*, 885.
(19) Davis, A. P.; Sheppard, D. N.; Smith, B. D. Development of synthetic membrane transporters for anions. *Chem. Soc. Rev.* **2007**, *36*, 348−357.
(20) Yano, M.; Tong, C. C.; Light, M. E.; Schmidtchen, F. P.; Gale, P. A. Calix [4] pyrrole-based anion transporters with tuneable transport properties. *Org. Biomol. Chem.* **2010**, *8*, 4356−4363.
(21) Tong, X.; Ao, Y.; Faas, G. C.; Nwaobi, S. E.; Xu, J.; Haustein, M. D.; Anderson, M. A.; Mody, I.; Olsen, M. L.; Sofroniew, M. V.; Khakh, B. S. Astrocyte Kir4. 1 ion channel deficits contribute to neuronal dysfunction in Huntington's disease model mice. *Nat. Neurosci.* **2014**, *17*, 694.
(22) Saha, T.; Hossain, M. S.; Saha, D.; Lahiri, M.; Talukdar, P. Chloride-mediated apoptosis-inducing activity of bis (sulfonamide) anionophores. *J. Am. Chem. Soc.* **2016**, *138*, 7558−7567.
(23) Fisher, M. G.; Gale, P. A.; Hiscock, J. R.; Hursthouse, M. B.; Light, M. E.; Schmidtchen, F. P.; Tong, C. C. 1, 2, 3-Triazole-strapped calix [4] pyrrole: a new membrane transporter for chloride. *Chem. Commun.* **2009**, *21*, 3017−3019.
(24) Li, X.; Shen, B.; Yao, X.-Q.; Yang, D. A small synthetic molecule forms chloride channels to mediate chloride transport across cell membranes. *J. Am. Chem. Soc.* **2007**, *129*, 7264−7265.
(25) Kubik, S. Anion recognition in aqueous media by cyclopeptides and other synthetic receptors. *Acc. Chem. Res.* **2017**, *50*, 2870−2878.
(26) Jentzsch, A. V.; Emery, D.; Mareda, J.; Nayak, S. K.; Metrangolo, P.; Resnati, G.; Sakai, N.; Matile, S. Transmembrane anion transport mediated by halogen-bond donors. *Nat. Commun.* **2012**, *3*, 905.
(27) Koulov, A. V.; Lambert, T. N.; Shukla, R.; Jain, M.; Boon, J. M.; Smith, B. D.; Li, H.; Sheppard, D. N.; Joos, J.-B.; Clare, J. P.; Davis, A. P. Chloride transport across vesicle and cell membranes by steroid-based receptors. *Angew. Chem., Int. Ed.* **2003**, *115*, 5081−5083.
(28) Valkenier, H.; Haynes, C. J. E.; Herniman, J.; Gale, P. A.; Davis, A. P. Lipophilic balance−a new design principle for transmembrane anion carriers. *Chem. Sci.* **2014**, *5*, 1128−1134.
(29) Lisbjerg, M.; Valkenier, H.; Jessen, B. M.; Al-Kerdi, H.; Davis, A. P.; Pittelkow, M. Biotin [6] uril Esters: Chloride-Selective Transmembrane Anion Carriers Employing C— H··· Anion Interactions. *J. Am. Chem. Soc.* **2015**, *137*, 4948−4951.
(30) Deng, G.; Dewa, T.; Regen, S. L. A synthetic ionophore that recognizes negatively charged phospholipid membranes. *J. Am. Chem. Soc.* **1996**, *118*, 8975−8976.
(31) Gale, P. A.; Pérez-Tomás, R.; Quesada, R. Acal systems. *Acc. Chem. Res.* **2013**, *46*, 2801−2813.
(32) Gale, P. A.; Tong, C. C.; Haynes, C. J. E.; Adeosun, O.; Gross, D. E.; Karnas, E.; Sedenberg, E. M.; Quesada, R.; Sessler, J. L. Octafluorocalix [4] pyrrole: a chloride/bicarbonate antiport agent. *J. Am. Chem. Soc.* **2010**, *132*, 3240−3241.
(33) Liu, P.-Y.; Li, S.-T.; Shen, F.-F.; Ko, W.-H.; Yao, X.-Q.; Yang, D. A small synthetic molecule functions as a chloride−bicarbonate dual-transporter and induces chloride secretion in cells. *Chem. Commun.* **2016**, *52*, 7380−7383.
(34) Moore, S. J.; Haynes, C. J. E.; González, J.; Sutton, J. L.; Brooks, S. J.; Light, M. E.; Herniman, J.; Langley, G. J.; Soto-Cerrato, V.; Pérez-Tomás, R.; Marques, I.; Costa, P. J.; Félix, V.; Gale, P. A. Chloride, carboxylate and carbonate transport by ortho-phenylenediamine-based bisureas. *Chem. Sci.* **2013**, *4*, 103−117.
(35) Hennig, A.; Fischer, L.; Guichard, G.; Matile, S. Anion−Macrodipole Interactions: Self-Assembling Oligourea/Amide Macrocycles as Anion Transporters that Respond to Membrane Polarization. *J. Am. Chem. Soc.* **2009**, *131*, 16889−16895.
(36) Sharma, G. V. M.; Manohar, V.; Dutta, S. K.; Sridhar, B.; Ramesh, V.; Srinivas, R.; Kunwar, A. C. Self-assembling cyclic tetrapeptide from alternating C-linked carbo-β-amino Acid [(S)-β-Caa] and α-aminoxy acid [(R)-Ama]: A selective chloride ion receptor. *J.Org.Chem* **2010**, *75*, 1087−1094.
(37) Yang, D.; Li, X.; Sha, Y.; Wu, Y. D. A Cyclic Hexapeptide Comprising Alternating α-Aminoxy and α-Amino Acids is a Selective Chloride Ion Receptor. *Chem.−Eur. J.* **2005**, *11*, 3005−3009.
(38) Yang, D.; Qu, J.; Li, W.; Zhang, Y.-H.; Ren, Y.; Wang, D.-P.; Wu, Y.-D. Cyclic hexapeptide of D, L-α-aminoxy acids as a selective receptor for chloride ion. *J. Am. Chem. Soc.* **2002**, *124*, 12410−12411.
(39) Krieger, V.; Ciglia, E.; Thoma, R.; Vasylyeva, V.; Frieg, B.; de Sousa Amadeu, N.; Kurz, T.; Janiak, C.; Gohlke, H.; Hansen, F. K. α-Aminoxy Peptoids: A Unique Peptoid Backbone with a Preference forcis-Amide Bonds. *Chem.−Eur. J.* **2017**, *23*, 3699−3707.
(40) Van Maarseveen, J. H.; Horne, W. S.; Ghadiri, M. R. Efficient Route to C 2 Symmetric Heterocyclic Backbone Modified Cyclic Peptides. *Org. Lett.* **2005**, *7*, 4503−4506.
(41) Horne, W. S.; Yadav, M. K.; Stout, C. D.; Ghadiri, M. R. Heterocyclic peptide backbone modifications in an α-helical coiled coil. *J. Am. Chem. Soc.* **2004**, *126*, 15366−15367.
(42) Seth Horne, W.; Olsen, C. A.; Beierle, J. M.; Montero, A.; Reza Ghadiri, M. Probing the Bioactive Conformation of an Archetypal Natural Product HDAC Inhibitor with Conformationally Homogeneous Triazole-Modified Cyclic Tetrapeptides. *Angew. Chem., Int. Ed.* **2009**, *48*, 4718−4724.
(43) Cai, J.; Sessler, J. L. Neutral CH and cationic CH donor groups as anion receptors. *Chem.Soc. Rev.* **2014**, *43*, 6198−6213.
(44) Mungalpara, D.; Stegmüller, S.; Kubik, S. A neutral halogen bonding macrocyclic anion receptor based on a pseudocyclopeptide with three 5-iodo-1, 2, 3-triazole subunits. *Chem. Commun.* **2017**, *53*, 5095−5098.
(45) Mungalpara, D.; Valkonen, A.; Rissanen, K.; Kubik, S. Efficient stabilisation of a dihydrogenphosphate tetramer and a dihydrogenpyrophosphate dimer by a cyclic pseudopeptide containing 1, 4-disubstituted 1, 2, 3-triazole moieties. *Chem. Sci.* **2017**, *8*, 6005−6013.
(46) Mullen, K. M.; Mercurio, J.; Serpell, C. J.; Beer, P. D. Exploiting the 1, 2, 3-triazolium motif in anion-templated formation of a bromide-selective rotaxane host assembly. *Angew. Chem., Int. Ed.* **2009**, *48*, 4781−4784.
(47) Nehra, A.; Yarramala, D. S.; Rao, C. P. A 1, 3-Capped Calix [4] Conjugate Possessing an Amine Moiety as an Anion Receptor: Reversible Anion Sensing Detected by Spectroscopy and Characterization of the Supramolecular Features by Microscopy. *Chem.−Eur. J.* **2016**, *22*, 8980−8989.

https://dx.doi.org/10.1021/acsomega.0c00438
ACS Omega 2020, 5, 16395−16405

(48) Ghorai, A.; Padmanaban, E.; Mukhopadhyay, C.; Achari, B.; Chattopadhyay, P. Design and synthesis of regioisomeric triazole based peptidomimetic macrocycles and their dipole moment controlled self-assembly. *Chem. Commun.* **2012**, *48*, 11975−11977.
(49) Ghorai, A.; Gayen, A.; Kulsi, G.; Padmanaban, E.; Laskar, A.; Achari, B.; Mukhopadhyay, C.; Chattopadhyay, P. Simultaneous parallel and antiparallel self-assembly in a triazole/amide macrocycle conformationally homologous to D-, L-α-amino acid based cyclic peptides: NMR and molecular modeling study. *Org. Lett.* **2011**, *13*, 5512−5515.
(50) Ghorai, A.; Samanth Reddy, K.; Achari, B.; Chattopadhyay, P. Rational Construction of Triazole/Urea Based Peptidomimetic Macrocycles as Pseudocyclo-β-peptides and Studies on Their Chirality Controlled Self-Assembly. *Org. Lett.* **2014**, *16*, 3196−3199.
(51) Kulsi, G.; Ghorai, A.; Achari, B.; Chattopadhyay, P. Design and synthesis of conformationally homogeneous pseudo cyclic peptides through amino acid insertion: investigations on their self assembly. *RSC Adv.* **2015**, *5*, 64675−64681.
(52) Li, X.; Wu, Y.-D.; Yang, D. α-Aminoxy acids: new possibilities from foldamers to anion receptors and channels. *Acc. Chem. Res.* **2008**, *41*, 1428−1438.
(53) Li, Y.; Flood, A. H. Pure C-H Hydrogen Bonding to Chloride Ions: A Preorganized and Rigid Macrocyclic Receptor. *Angew. Chem., Int. Ed.* **2008**, *47*, 2649−2652.
(54) Li, Y.; Flood, A. H. Strong, Size-Selective, and Electronically Tunable C− H··· Halide Binding with Steric Control over Aggregation from Synthetically Modular, Shape-Persistent [3 4] Triazolophanes. *J. Am. Chem. Soc.* **2008**, *130*, 12111−12122.
(55) Hua, Y.; Flood, A. H. Click chemistry generates privileged CH hydrogen-bonding triazoles: the latest addition to anion supramolecular chemistry. *Chem. Soc. Rev.* **2010**, *39*, 1262−1271.
(56) Kumar, A.; Pandey, P. S. Anion recognition by 1, 2, 3-triazolium receptors: application of click chemistry in anion recognition. *Org. Lett.* **2008**, *10*, 165−168.
(57) Verkman, A. S.; Takla, R.; Sefton, B.; Basbaum, C.; Widdicombe, J. H. Quantitative fluorescence measurement of chloride transport mechanisms in phospholipid vesicles. *Biochemistry* **1989**, *28*, 4240−4244.
(58) Rostovtsev, V. V.; Green, L. G.; Fokin, V. V.; Sharpless, K. B. A stepwise huisgen cycloaddition process: copper (I)-catalyzed regioselective "ligation" of azides and terminal alkynes. *Angew. Chem., Int. Ed.* **2002**, *41*, 2596−2599.
(59) Tornøe, C. W.; Christensen, C.; Meldal, M. Peptidotriazoles on solid phase:[1, 2, 3]-triazoles by regiospecific copper (I)-catalyzed 1, 3-dipolar cycloadditions of terminal alkynes to azides. *J.Org.Chem* **2002**, *67*, 3057−3064.
(60) Sannigrahi, A.; Chall, S.; Jawed, J. J.; Kundu, A.; Majumdar, S.; Chattopadhyay, K. Nanoparticle Induced Conformational Switch Between α-Helix and β-Sheet Attenuates Immunogenic Response of MPT63. *Langmuir* **2018**, *34*, 8807−8817.
(61) Sannigrahi, A.; Mullick, D.; Sanyal, D.; Sen, S.; Maulik, U.; Chattopadhyay, K. Effect of Ergosterol on the Binding of KMP-11 with Phospholipid Membranes: Implications in Leishmaniasis. *ACS Omega* **2019**, *4*, 5155−5164.
(62) Sannigrahi, A.; Maity, P.; Karmakar, S.; Chattopadhyay, K. Interaction of KMP-11 with phospholipid membranes and its implications in leishmaniasis: effects of single tryptophan mutations and cholesterol. *J. Phys. Chem. B* **2017**, *121*, 1824−1834.
(63) Sannigrahi, A.; Nandi, I.; Chall, S.; Jawed, J. J.; Halder, A.; Majumdar, S.; Karmakar, S.; Chattopadhyay, K. Conformational switch driven membrane pore formation by Mycobacterium secretory protein MPT63 induces macrophage cell death. *ACS Chem. Biol.* **2019**, *14*, 1601−1610.
(64) Bhanja, P.; Mishra, S.; Manna, K.; Mallick, A.; Das Saha, K.; Bhaumik, A. Covalent organic framework material bearing phloroglucinol building units as a potent anticancer agent. *ACS Appl. Mater. Interfaces* **2017**, *9*, 31411−31423.
(65) Nandi, R.; Mishra, S.; Maji, T. K.; Manna, K.; Kar, P.; Banerjee, S.; Dutta, S.; Sharma, S. K.; Lemmens, P.; Saha, K. D.; Pal, S. K. A novel nanohybrid for cancer theranostics: folate sensitized Fe_2O_3 nanoparticles for colorectal cancer diagnosis and photodynamic therapy. *J. Mater. Chem. B* **2017**, *5*, 3927−3939.
(66) Das, S. K.; Mishra, S.; Manna, K.; Kayal, U.; Mahapatra, S.; Saha, K.; Dalapati, S.; Das, G. P.; Mostafa, A. A.; Bhaumik, A. A new triazine based π-conjugated mesoporous 2D covalent organic framework: its in vitro anticancer activities. *Chem. Commun.* **2018**, *54*, 11475−11478.

https://dx.doi.org/10.1021/acsomega.0c00438
ACS Omega 2020, 5, 16395−16405